Avian Research 14 (2023) 100097

Contents lists available at ScienceDirect

Avian Research

journal homepage: www.keaipublishing.com/en/journals/avian-research

Evolutionary relationships of mitogenomes in a recently radiated Old World avian family

Wenqing Zang [a,b], Zhiyong Jiang [a,b], Per G.P. Ericson [c], Gang Song [a], Sergei V. Drovetski [d,e], Takema Saitoh [f], Fumin Lei [a,b,g], Yanhua Qu [a,b,*]

[a] Key Laboratory of Zoological Systematics and Evolution, Institute of Zoology, Chinese Academy of Sciences, Beijing, China
[b] College of Life Sciences, University of Chinese Academy of Sciences, Beijing, China
[c] Department of Bioinformatics and Genetics, Swedish Museum of Natural History, PO Box 50007, SE-104 05, Stockholm, Sweden
[d] Laboratories of Analytical Biology, National Museum of Natural History, Smithsonian Institution, Washington, DC 20004, USA
[e] Current address: U.S. Geological Survey, Eastern Ecological Science Center at Patuxent Research Refuge, Laurel, MD 20708, USA
[f] Yamashina Institute for Ornithology, Abiko, Chiba, Japan
[g] Center for Excellence in Animal Evolution and Genetics, Chinese Academy of Sciences, Kunming, 650223, China

ARTICLE INFO

Keywords:
Incomplete lineage sorting
Mitochondrial genome
Mountain specialists
Radiation

ABSTRACT

Environmentally heterogeneous mountains provide opportunities for rapid diversification and speciation. The family Prunellidae (accentors) is a group of birds comprising primarily mountain specialists that have recently radiated across the Palearctic region. This rapid diversification poses challenges to resolving their phylogeny. Herein we sequenced the complete mitogenomes and estimated the phylogeny using all 12 (including 28 individuals) currently recognized species of Prunellidae. We reconstructed the mitochondrial genome phylogeny using 13 protein-coding genes of 12 species and 2 Eurasian Tree Sparrows (*Passer montanus*). Phylogenetic relationships were estimated using a suite of analyses: maximum likelihood, maximum parsimony and the coalescent-based SVDquartets. Divergence times were estimated by implementing a Bayesian relaxed clock model in BEAST2. Based on the BEAST time-calibrated tree, we implemented an ancestral area reconstruction using RASP v.4.3. Our phylogenies based on the maximum likelihood, maximum parsimony and SVDquartets approaches support a clade of large-sized accentors (subgenus *Laiscopus*) to be sister to all other accentors with small size (subgenus *Prunella*). In addition, the trees also support the sister relationship of *P. immaculata* and *P. rubeculoides* + *P.atrogularis* with 100% bootstrap support, but the relationships among the remaining eight species in the *Prunella* clade are poorly resolved. These species cluster in different positions in the three phylogenetic trees and the nodes are often poorly supported. The five nodes separating the seven species diverged simultaneously within less than half million years (i.e., between 2.71 and 3.15 million years ago), suggesting that the recent radiation is likely responsible for rampant incomplete lineage sorting and gene tree conflicts. Ancestral area reconstruction indicates a central Palearctic region origin for Prunellidae. Our study highlights that whole mitochondrial genome phylogeny can resolve major lineages within Prunellidae but is not sufficient to fully resolve the relationship among the species in the *Prunella* clade that almost simultaneously diversify during a short time period. Our results emphasize the challenge to reconstruct reliable phylogenetic relationship in a group of recently radiated species.

1. Introduction

Mountain regions frequently exhibit greater biodiversity than lowland due to their environmental heterogeneity along the elevation gradients, which increase conservation importance of mountains despite their small geographic areas (Lafon, 2004). Although mountains cover only 16.5–27% of the land area, half of the currently recognized biodiversity hot spots consists of mountain regions (Kohler and Maselli, 2009; Fjeldså et al., 2012). To a large extent, high species richness in mountains has been attributed to physiographical (i.e., topography) and environmental heterogeneity (Kreft and Jetz, 2007; Ruggiero and Hawkins, 2008; Fjeldså et al., 2012; Ghalambor et al., 2016), which has facilitated

* Corresponding author. Key Laboratory of Zoological Systematics and Evolution, Institute of Zoology, Chinese Academy of Sciences, Beijing, China.
E-mail address: quyh@ioz.ac.cn (Y. Qu).

https://doi.org/10.1016/j.avrs.2023.100097
Received 4 February 2023; Received in revised form 20 March 2023; Accepted 22 March 2023
Available online 31 March 2023

volatility of range shifts and adaptation leading to speciation. This exploratory radiation has been considered to play a fundamental role in generating montane biodiversity.

A proper assessment of the evolution and diversification of montane taxa requires a reliable phylogenetic relationship. However, phylogeny reconstruction for rapidly radiating groups has been proved to be difficult (Prum et al., 2015; Chen et al., 2015; Irisarri and Meyer, 2016; Tarver et al., 2016). This is because a rapid diversification generates multiple species during a short time period that results in incomplete lineage sorting due to shared ancestral polymorphism (Maddison and Knowles, 2006; Oliver, 2013). Mitochondrial genome, in contrast to nuclear coding genes, is characterized by a relatively high rate of nucleotide substitutions, lack of recombination and matrilineal inheritance. The potential of mitochondrial genome for understanding the mechanisms of speciation and factors affecting phylogeny reconstruct during rapid diversification is thus excellent, and it has been widely applied for species identification (i.e., barcoding), phylogeography and phylogenetics (Duchéne et al., 2011; González-Castellano et al., 2020; da Silva et al., 2020; Yu et al., 2021).

Accentors (Prunellidae) form a close-knit group with 12 currently recognized species (Gill et al., 2022). The entire family is distributed across the Palearctic. Many accentors live in mountains and these species differ in their elevation and habitat distributions from high alpine to lower montane forest habitats. Most accentors are distributed in the Sino-Himalayan Mountains of the central Palearctic, including the Himalayas, Tibet and mountains of south-central China. These partial disjunctions can be related to the patchiness of the preferred habitat, as most accentors breed in alpine environments and near the upper timberline in high mountains. Previous molecular phylogenies of the accentors have utilized one or two mitochondrial and/or a few nuclear genes, but the relationships among several of the species have proven difficult to resolve (Drovetski et al., 2013; Liu et al., 2017).

Herein we aim at resolving a complete species phylogeny of 12 currently recognized species based on 13 protein-coding mitochondria genes. We reconstruct phylogenetic trees obtained with maximum likelihood, maximum parsimony and SVDquartets approaches, in order to evaluate the effect of different tree reconstruction methods on resolving Prunellidae phylogeny. As this work provides the most inclusive mitochondrial genome phylogeny of the Prunellidae to date, we want to test if more genes would provide a better resolution that a few genes used in previous studies, that is, more is better. As our phylogenies based on different tree reconstruction approaches support two major clades (subgenera *Laiscopus* and *Prunella*), but remain unresolved for the seven species that diverge simultaneously at the same time. We conclude that it is difficult to fully resolve the phylogenetic relationships in Prunellidae even when using the whole mitochondrial genome, which highlights the challenge of reconstructing a reliable phylogeny for the groups that have undergone rapid diversifications.

2. Methods

2.1. Taxon sampling

In the study, we included all traditionally recognized accentor species in Prunellidae (Drovetski et al., 2013; Liu et al., 2017). The Arabian Accentor (*P. fagani*) was previously treated as a distinct species (Dickinson, 2003; Gill and Donsker, 2016), but was recently merged with Radde's Accentor (*P. ocularis*; Gill et al., 2022). As the *P. fagani* is geographically widely separate from the *P. ocularis*, we herein treated *P. fagani* and *P. ocularis* as two taxonomic units. We included two or three individuals for most species except the two narrow ranged taxa, i.e., Mongolian Accentor (*P. koslowi*) and Black-throated Accentor (*P. atrogularis*), for which only a single individual for each species was used. In total, we included 30 individuals (28 accentors and two Eurasian Tree Sparrow, *Passer montanus*) in this study (Appendix Table S1).

2.2. DNA extraction, library preparation and sequencing information

DNA from the frozen tissue samples and museum toe pad samples was extracted using the Qiagen QIAamp DNA Mini Kit according to the manufacturer's protocol and sequenced in the Annuo Genomics (Beijing), Berry Genomic Institute (Beijing) and SciLife Laboratories (Stockholm). The sequencing libraries for fresh tissues were prepared using the Illumina TruSeq PCA-free (190/350 bp) kit and were sequenced on an Illumina Novaseq platform. The libraries from museum specimens were prepared using the protocol published by Meyer and Kircher (2010). Skin library could only be successfully sequenced for one of two individuals of *P. fagani* and we used this sample for downstream analysis. All samples were sequenced to a mean coverage of 20 × (Appendix Table S1).

2.3. Assemble mitochondria genome

Raw sequenced reads from accentor individuals and two Eurasian Tree Sparrow individuals (provided as outgroup) were cleaned following these filtering steps: 1) removing adapter, 2) removing low-quality reads, i.e., reads with the proportion of "N" > 3%, reads with >50% low-quality bases (<3). Raw reads from the sequencing of museum specimen were cleaned by same procedure except deleting 5 bp from both ends in order to reduce the influence of DNA degradation. We assembled the mitochondrial genome from the resequenced data for an individual of Rufous-breasted Accentor (*P. strophiata*) using Mitoz (Meng et al., 2019), and the protein-coding genes, tRNA and rRNA were annotated using Mitos2 (Bernt et al., 2013). The mitochondrial genome map was drawn using Proksee (https://proksee.ca/). Using this assembled mitochondrial genome sequence of *P. strophiata* as reference, we mapped raw reads of other accentor individuals and generated the consensus sequences for each of them.

2.4. Phylogenetic analyses

The phylogenetic analyses were performed based on 13 protein-coding genes of accentors and Eurasian Tree Sparrows. All sequences were aligned using Mafft v.7.471 (Katoh and Standley, 2013). Phylogenetic relationships were estimated with a suite of analyses: maximum likelihood, maximum parsimony and the coalescent-based SVDquartets analyses (Chifman and Kubatko, 2014, 2015). Maximum likelihood trees were reconstructed using IQ-TREE (Nguyen et al., 2015). We applied the "–m TEST" option to find the best substitution model (GTR + F + I + G4) for the alignment. Branch supports for the maximum likelihood tree were calculated using the ultrafast bootstrap option (Hoang et al., 2018) implemented in the IQ-TREE. We estimated maximum parsimony and SVDquartets analyses using PAUP* v.4.0a169 (Swofford, 2021).

2.5. Estimating time of divergence

We assessed rapid cladogenesis by estimating relative timings of divergence in major lineages using 13 protein-coding genes. Divergence time estimates were obtained by implementing a Bayesian relaxed clock model in BEAST2 (Bouckaert et al., 2014) based on the whole mitochondrial genome sequences. We ran Markov chain Monte Carlo chains for 100 million generations (sampling every 1000 generations) using a relaxed lognormal distribution for the molecular clock model and assuming a birth-death speciation process for the tree prior. The tree was calibrated using a molecular clock of 1.8% per million years (Lerner et al., 2011). We checked for convergence between runs and analysis performance using Tracer v.1.5 and accepted the results if the values of the estimated sample size (ESS) were larger than 200, suggesting little autocorrelation between samples. The resulting trees were combined in TreeAnnotator v.1.7.5 (Drummond et al., 2012) and the consensus tree with the divergence time was visualized in FigTree v.1.4.4. (Rambaut, 2012). Mean values and 95% confidence intervals of ages of these runs were estimated after a burn-in phase of the first five million generations.

2.6. Ancestral area reconstruction

Based on the time-calibrated tree estimated in BEAST, we reconstructed ancestral areas for accentors using RASP v.4.3 (Yu et al., 2010, 2015). Following Drovetski et al. (2013), the different Prunellidae species could be roughly placed into five geographic regions: western Palearctic (A), southwest Asia (B), central Palearctic plateau (C), eastern Palearctic island chain (D) and north-eastern Palearctic (E) according to the ranges specified by IUCN (https://www.iucnredlist.org/). We estimated multiple dispersal events (Appendix Table S2) taking the connectivity between the geographic regions into account (Zhang et al., 2021). We tested six models, dispersal–extinction–cladogenesis (DEC) model, DEC + J, dispersal vicariance analysis (DIVA) like model, DIVALIKE + J, BayArea-like model and BayArea-like + J, using Bayesian and likelihood evolutionary analyses built-in in the BioGeoBEARS v.1.1.1 (Matzke, 2013; 2014). The most likely model was selected using the Akaike's information criterion with correction weights (AICc_wt) (Appendix Table S3). Based on the selected model, we estimated the most likely ancestral areas using BioGeoBEARS (Appendix Fig. S1).

3. Results

3.1. Mitochondrial genomes of the accentors

The complete mitochondrial genome of *P. strophiata* contained a total length of 16,830 bp. The genome included 13 protein-coding genes (*nd1–6*, *nd4l*, *cox1–3*, *cytb*, *atp6* and *atp8*), 22 tRNA genes, 2 rRNA genes and the control region (Appendix Fig. S2, Appendix Table S4). The protein-coding genes range in size from 168 bp (*atp8*) to 1818 bp (*nd5*), with a total length of 11,389 bp, tRNAs vary from 65 bp (i.e., tRNA-GCT) to 75 bp (i.e., tRNA-TAA) in size, with a total length of 1543 bp. The lengths of small encoding subunit 12S rRNA and large subunit 16S rRNA are 976 bp and 1587 bp, respectively. We also identified a 1047 bp control region. Using the mitochondrial genome of *P. strophiata* as a reference, we generated mitochondrial genome sequence for each of remaining 27 accentors. Of a total of 28 mitochondrial genomes across 12 accentor species, the average sequence divergence of the 13 protein-coding genes was 12.4% with a range between 8.6% (cyt*b*) and 16.5% (*nd2*). The genes with the largest number of parsimony-informative sites were *nd2* (35.7%), *nd1* (32.3%) and *nd3* (31.6%; Table 1).

3.2. Phylogenetic relationship of accentors inferred using mitochondrial genome

The phylogenetic trees inferred from different approaches showed a roughly similar topology and differed only in the placement of a few species (Fig. 1). In all trees, the 12 accentors were monophyletic relative to the Eurasian Tree Sparrow. They were divided into two clades corresponding to subgenera *Laiscopus* and *Prunella* (following Stepanyan, 2003). Both clades received 100% bootstrap support in maximum-likelihood, maximum parsimony and SVDquartets trees. The *Laiscopus* clade comprised Altai Accentor (*P. himalayana*) and Alpine Accentor (*P. collaris*), while the *Prunella* clade consisted of the remaining ten species. Within the *Prunella* clade, Maroon-backed Accentor (*P. immaculata*) represented the earliest split, followed by a lineage of a pair Robin Accentor (*P. rubeculoides*) and *P. atrogularis* that was a sister to the clade consisted of remaining species. This topology is supported in the maximum-likelihood and maximum parsimony trees with 100% bootstrap support, but in the SVDquartets tree *P. immaculata* clustered with *P. rubeculoides* + *P. atrogularis* and these three species then formed the sister lineage to the remaining accentors within *Prunella* clade (Fig. 1).

There was also notable discordance in the positions of several species within the *Prunella* clade in the three phylogenetic trees. First, three individuals of the Dunnock (*P. modularis*) were recovered as monophyletic in the maximum likelihood and parsimony trees with 100% bootstrap support. However, in the SVDquartets tree, one individual of *P. modularis* clustered with one Siberian Accentor (*P. montanella*) individual, while other two *P. modularis* individuals clustered with *P. koslowi* + *P. fulvescens*, although these subclades received 84% and 61% bootstrap supports, respectively. In the SVDquartets tree, the two *P. montanella* individuals grouped with *P. ocularis* + *P. fagani* with 52% bootstrap support. Second, two individuals of *P. rubida* were recovered as monophyletic in the maximum likelihood and parsimony trees but not in the SVDquartets tree. Third, *P. montanella* clustered with *P. rubida* in the maximum likelihood and parsimony trees, but grouped with *P. ocularis* + *P. fagani* in the SVDquartets tree. In the latter tree, *P. fulvescens* + *P. koslowi* clustered with two individuals of *P. modularis*, and then clustered together with *P. ocularis* + *P. fagani*, and two individuals of *P. montanella*. The clade with these species had 62% bootstrap support. In the maximum parsimony tree, *P. fulvescens* + *P. koslowi*, *P. montanella* + *P. rubida*, *P. ocularis* + *P. fagani* and *P. strophiata* formed four polyphyletic lineages with 70% bootstrap support. Altogether, our phylogenies inferred from three different approaches for tree reconstruction congruently supported the division of the accentors into two major clades (*Laiscopus* and *Prunella*), as well as two basal positions of *P. immaculata* and *P. rubeculoides* + *P. atrogularis*. However, the relationships among the remaining species vary under different phylogenetic inference approaches, suggesting that the relationships of these species in the *Prunella* clade are hard to resolve with mitochondrial data.

Table 1
Thirteen protein-coding genes used in the phylogenetic inference.

Name	Length (bp)	Numbers of parsimony-informative sites	Percentage of parsimony-informative sites (%)	Sequence divergence (%)
nd1	971	314	32.34	12.40
nd2	1041	372	35.73	16.50
cox1	1551	383	24.69	10.80
cox2	684	195	28.51	9.20
atp8	168	46	27.38	15.60
atp6	683	206	30.16	14.00
cox3	785	189	24.08	9.80
nd3	351	111	31.62	12.90
nd4l	297	92	30.98	14.90
nd4	1378	399	28.96	13.00
nd5	1818	536	29.48	11.20
cytb	1143	289	25.28	8.60
nd6	519	158	30.44	12.80

3.3. Divergence time estimate and biogeography

The topology inferred from BEAST is largely similar to the phylogeny inferred by maximum likelihood but differs in the relative positions of *P. fulvescens* + *P. koslowi*, which is clustered with *P. strophiata* and subsequently forms the sister lineage to *P. rubida* + *P. montanella* in the BEAST tree. In the maximum likelihood tree, *P. fulvescens* + *P. koslowi* firstly clustered with *P. modularis*, and then grouped with *P. ocularis* + *P. fagani* (Figs. 1 and 2). Using a molecular clock based on a divergence time of 1.8% per million years between taxa for the mitochondrial DNA (Lerner et al., 2011), we showed that the accentors split from their most recent common ancestor at 16.41 million years ago (Ma) with an interval of the 95% highest posterior density (HPD) of 14.99–17.91 Ma (Fig. 2). The split between the *Laiscopus* and *Prunella* clades occurred at approximately 7.28 Ma (95% HPD, 6.78–7.79 Ma). The subsequent radiations within the *Laiscopus* and *Prunella* clades occurred around 3.0 Ma (95% HPD, 2.75–3.27 Ma) and 5.12 Ma (95% HPD, 4.78–5.55 Ma), respectively. Within the *Prunella* clade, the first two splits leading the three species (*P. immaculata* and *P. rubeculoides* + *P. atrogularis*) happened at 5.12 and 4.2 Ma, respectively (*P. immaculata*, 95% HPD, 4.78–5.55 Ma; *P. rubeculoides* + *P. atrogularis*, 95% HPD, 3.95–4.45 Ma). Subsequently, the remaining *Prunella* species were succeeded by a set of cladogenetic events by four simultaneous splits at 2.71–3.15 Ma. For example,

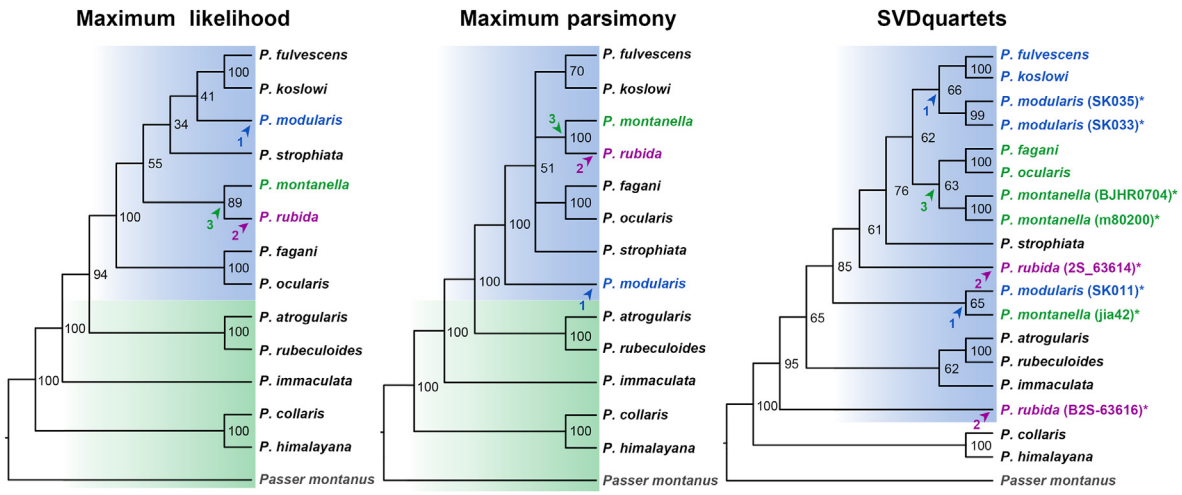

Fig. 1. The maximum-likelihood tree (generated with IQ-TREE) and maximum parsimony and SVDquartets trees (tree generated from PAUP) derived from mitochondrial genomes of 28 accentors representing 12 currently accentor species and two Eurasian Tree Sparrows. The maximum-likelihood tree of accentors is on the left, while the maximum parsimony tree is shown on the middle, and the SVDquartets tree is on the right. All three trees support monophyly of Prunellidae and reciprocal monophyly of the subgenera *Prunella* and *Laiscopus*. Within *Prunella*, three phylogenetic trees also support the basal splits of *P. immaculata* and *P. rubeculoides* + *P. atrogularis*, but the relationships among the remaining species in the *Prunella* clade are unresolved. Three numbers in different colors marked the three examples of topology incongruence described in the Results.

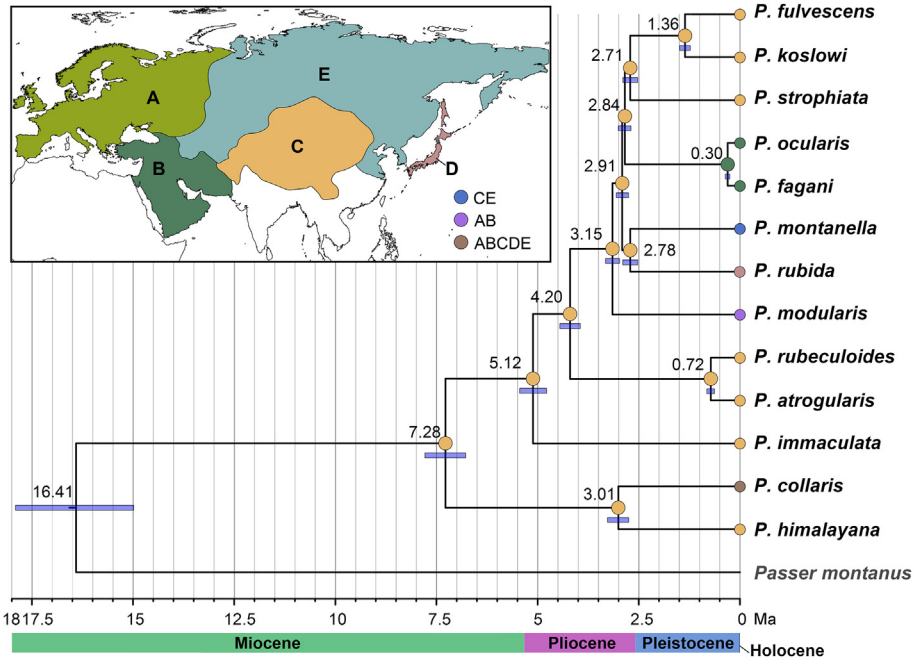

Fig. 2. The divergence times of Prunellidae and ancestral area reconstruction using 13 protein-coding genes in the complete mitochondrial genome. Nodal labels indicate the time to the most recent common ancestor (TMRCA). The 95% HPD intervals are represented by blue bars and the scale shows Ma (million years ago). The ancestral area reconstruction is estimated using the BayArea-like model generated in RASP. The estimated ancestral areas are colored according to the five geographic regions defined as western Palearctic (A), southwest Asia (B), central Palearctic (C), eastern Palearctic island chain (D), northern part of eastern Palearctic (E). The colors of the dots on the nodes show the most likely ancestral area estimated by BioGeoBEARS and indicate that the Prunellidae originated from the central Palearctic region. Insert: biogeographic areas used in the ancestral area reconstruction.

P. modularis split at 3.15 Ma and was followed by *P. rubida* + *P. montanella* splitting at 2.91 Ma, *P. fagani* + *P. ocularis* splitting at 2.84 Ma, and *P. fulvescens* + *P. koslowi* splitting from *P. strophiata* at 2.71 Ma. This time period is congruent with Pliocene-Pleistocene boundary.

Biogeographic model showed the BayArea-like model received the highest support with AICc_Wt close to one (Appendix Table S3). Based on this model, we estimated ancestral areas across the time-calibrated tree (Appendix Fig. S1). There are three species that are sympatric in the Himalayan regions in central Palearctic, *P. rubiculoides*, *P. immaculata*, *P. strophiata*. Two species, *P. atrogularis* and *P. koslowi*, are endemic to the central Palearctic mountains, and two species, *P. fulvescens* and *P. himalayana*, are distributed across the Himalayan region and central Palearctic mountains. Two taxa, *P. fagani* and *P. ocularis*, are restricted to western Palearctic. *P. rubida* is endemic to Pacific Islands, and *P. montanella* is distributed across the central and eastern Palearctic, and *P. collaris* is distributed across all regions (Fig. 2).

4. Discussion

4.1. Phylogenetic relationships of accentors

Our work describes the mitochondrial genomes of accentors for the first time. These 28 genomes from all 12 species from entire Prunellidae family increase the available sequence resources for Passerine birds in publicly available databases. Gene content and order of our mitochondrial genomes are the same as the other passerines with known

mitochondrial genome (i.e., Eurasian Tree Sparrows). Based on these newly generated mitochondrial genomes, we present the first complete mitochondrial genome species tree of the Prunellidae, which consistently recovered a phylogeny with high supports for major clades using several different approaches. The topologies supported the monophyly of Prunellidae and two major clades within the family: *Prunella* and *Laiscopus*. The Prunellidae consists of a single genus (*Prunella*) and 12 species according to IOC World Bird list (Gill et al., 2022). Two large, high alpine species (*P. collaris* and *P. himalayana*) form a clade that is distinct from a clade of all other, smaller accentors that are associated with shrubs or scrub habitats (Hatchwell, 2005). The distinct ecological and morphological differences between the two clades were used to recognize them as distinct subgenera, *Laiscopus* and *Prunella* (Stepanyan, 2003; Drovetski et al., 2013). Our study based on whole mitochondrial genome data and the previous studies (Drovetski et al., 2013; Liu et al., 2017) identifies genetic differences between the two clades and supports this taxonomic treatment.

Within the *Prunella* clade, our study shows that three species, *P. immaculata*, *P. rubeculoides* and *P. atrogularis*, diverge early from the lineage leading to all other small accentors. Their relationships among each other and relative to the remaining species in the *Prunella* clade are well supported in all tree topologies regardless of analytical approach. However, different methods recovered different tree topologies within the *Prunella* clade. Three species in particular, *P. modularis*, *P. strophiata* and *P. rubida*, occur in different positions but the bootstrap supports for these relationships are low. The poorly resolved relationships within the whole clade have also been observed in previous phylogenetic studies based on a few mitochondrial and nuclear genes (Drovetski et al., 2013; Liu et al., 2017). The most likely explanation for the lack of resolution in the phylogenetic relationship of these species is likely because of their divergence in a close succession at the Pliocene-Pleistocene boundary. Both the short branches recovered by the different phylogenetic trees and the low support values associated with these nodes across all phylogenetic reconstructions are consistent with a rapid radiation at the origin of the *Prunella* clade. This would have contributed to high levels of sharing standing genetic variation among these species and to incomplete lineage sorting, making it difficult to disentangle the relationships between the branches in the phylogenetic trees (Svardal et al., 2021). Interestingly, we found that *P. atrogularis* clustered with *P. rubeculoides* in the phylogenies reconstructed in this study. By contrast, this species was grouped with *P. fagani/P. ocularis* in the previous studies (Drovetski et al., 2013; Liu et al., 2017), as well as in the phylogenomic trees inferring using same individuals from the 12 species. This topology incongruence is likely due to a secondary gene flow between *P. atrogularis* and *P. rubeculoides* (Jiang et al., unpublished), which likely still remains in the mitochondrial genome but less in the nuclear genome (i.e., Chan and Levin, 2005; Bachtrog et al., 2006).

Analyses of the mitochondrial genome have made an important contribution to resolving phylogenetic relationships of vertebrates and invertebrates (Duchéne et al., 2011; González-Castellano et al., 2020; da Silva et al., 2020; Yu et al., 2021). Nevertheless, incomplete lineage sorting has led to persistent uncertainty in estimates of the evolutionary timescales and relationships of rapidly radiated groups (Philippe et al., 2011; Mitchell et al., 2017). Even when using several different analytical approaches and the whole mitochondrial genome, the phylogenetic relationships among many *Prunella* species remain incompletely unresolved. Our study thus highlights the limitation in inferring phylogenetic relationships relying solely on this single marker, particularly for groups prone to introgression (Edwards et al., 2016).

4.2. Evolution and biogeography of accentors

The distribution of the most Prunellidae species mostly coincides with the higher mountains in the Palearctic region. Our analyses based on the mitochondrial genome phylogeny suggest a Miocene origin of Prunellidae in the central Palearctic regions at approximately 14 million years ago. The major division between alpine species (*Laiscopus* clade) and species associated with shrubs (*Prunella* clade) and the initial diversification events within the latter clade took place within the central Palearctic region in the Miocene and Pliocene. Accentors colonized other parts of the Palearctic region during the Pliocene-Pleistocene transition. Interestingly, we found that the youngest split between the two previously recognized species (*P. fagani* and *P. ocularis*) occurred at 0.30 Ma, which is much younger than the within-species divergence of *P. collaris* (1.11 Ma). This may explain why *P. fagani* has recently been merged with *P. ocularis*. *P. collaris* is widely distributed across the Palearctic region, and the populations living in different mountains have obviously been separated for a long time. The divergence time inferred in our study is more similar to that in Drovetski et al. (2013) but slightly younger than that in Liu et al. (2017). This is likely because of the molecular clock used in different studies. Nevertheless, all these studies consistently show that the common ancestor of the accentors lived in the Sino-Himalayan Mountains, or in these mountains together with central Asia-Mongolia in the Miocene and Pliocene (Drovetski et al., 2013; Liu et al., 2017). Altogether, the spatially heterogeneous mountainous environments and climatic fluctuations during the Miocene and Pliocene may have facilitated vicariate events and led to a rapid speciation and divergence of the accentors.

This rapid diversification of the Prunellidae is likely an evolutionary response to the ecosystem shift driven by environmental and climatic changes across vast tracts of mountains of Europe and Asia. First, the orogeny and mountain formation in the Palearctic region, especially during the Miocene and Pliocene, provided diversified ecological environments and created novel ecological niches (Miao et al., 2012; Deng et al., 2014; Favre et al., 2015) that led to rapid colonization and expansion of many montane species. The heterogeneous mountain landscape caused fragmentation of the colonizing species, which in turn led to a rapid allopatric diversification (Esquerré et al., 2019). Second, the Pleistocene glacial cycles provided multiple opportunities for downslope expansion and secondary contact of species that were previously isolated on mountain tops (Wang et al., 2013; Zhao et al., 2019). It has been shown that cold-adapted birds expanded into lowlands during glacial periods and then moved uphill to mountain tops during warm interglacials (e.g., Zhao et al., 2012; Zhang et al., 2012; Drovetski et al., 2018; Song et al., 2018, 2020). The results of our study of the accentors agree with those of other avian species and demonstrate how the climatic perturbations during the Pliocene-Pleistocene have facilitated avian diversification and adaptive evolution across the mountains in the Palearctic region in response to both environmental change and the novel ecological opportunities.

5. Conclusion

Using reconstruction of the Prunellidae phylogeny obtained by analyzing mitochondrial whole genome data with several analytical approaches and a time-calibrated tree, we demonstrate an important Pliocene-Pleistocene radiation in the mountain ecosystems in Palearctic region. The uplift of large mountainous areas across the Palearctic region gave rise to new ecological niches, which provide opportunities for colonization and speciation. During the Pleistocene glaciations, these species likely shifted to lower elevations and may have gotten in secondary contact. We conclude that rapid diversification driven by shifting species distributions due to climatic oscillations complicates phylogenetic reconstruction of the accentors.

Funding

This research was funded by the National Natural Science Foundation of China (NSFC32020103005), the Third Xinjiang Scientific Expedition and Research (XIKK) (2022xjkk0205) and Second Tibetan Plateau Scientific Expedition and Research (2019QZKK0501).

Authors' contributions

WZ, PGPE and YQ conceptualized the idea of the study. GS, SVD, TS and FL contribute samples. WZ, ZJ and PGPE performed analysis and visualization. WZ, PGPE and YQ wrote the paper. All authors read and approved the final manuscript.

Ethics statement

Not applicable.

Declaration of competing interest

The authors declare that they have no competing interest.

Acknowledgements

Samples for this study were kindly provided by the Burke Museum and Yale Peabody Museum, USA, Natural History Museum of Denmark, Copenhagen, and Natural History Museum of Norway, Oslo. We are particularly grateful to Jon Fjeldså, Kristof Zyskowski and Sharon Birks for their assistance with this study. We thank Martin Irestedt for extracting DNA and building sequence library for the sample of *Prunella fagani* for which only a museum skin was available.

Appendix A. Supplementary data

Supplementary data to this article can be found online at https://doi.org/10.1016/j.avrs.2023.100097.

References

Bachtrog, D., Thornton, K., Clark, A., Andolfatto, P., 2006. Extensive introgression of mitochondrial DNA relative to nuclear genes in the *Drosophila yakuba* species group. Evolution 60, 292–302.
Bernt, M., Donath, A., Jühling, F., Externbrink, F., Florentz, C., Fritzsch, G., et al., 2013. MITOS: improved de novo metazoan mitochondrial genome annotation. Mol. Phylogenet. Evol. 69, 313–319.
Bouckaert, R.R., Heled, J., Kuehnert, D., Vaughan, T.G., Wu, C.H., Xie, D., et al., 2014. Beast 2: a software platform for Bayesian evolutionary analysis. PLoS Comput. Biol. 10, e1003537.
Chan, K.M.A., Levin, S., 2005. Leaky prezygotic isolation and porous genome: rapid introgression of maternally inherited DNA. Evolution 59, 720–729.
Chen, M.Y., Liang, D., Zhang, P., 2015. Selecting question-specific genes to reduce incongruence in phylogenomics: a case study of jawed vertebrate backbone phylogeny. Syst. Biol. 64, 1104–1120.
Chifman, J., Kubatko, L.S., 2014. Quartet inference from SNP data under the coalescent model. Bioinformatics 30, 3317–3324.
Chifman, J., Kubatko, L.S., 2015. Identifiability of the unrooted species tree topology under the coalescent model with time-reversible substitution processes, site-specific rate variation, and invariable sites. J. Theor. Biol. 374, 35–47.
da Silva, F.S., Cruz, A.C.R., de Almeida Medeiros, D.B., Silva, S.P., Nunes, M.R.T., Martins, L.C., et al., 2020. Mitochondrial genome sequencing and phylogeny of *Haemagogus albomaculatus, Haemagogus leucocelaenus, Haemagogus spegazzinii*, and *Haemagogus tropicalis* (Diptera: Culicidae). Sci. Rep. 10, 16948.
Deng, X.D., Li, J.W., Vasconcelos, P.M., Cohen, B.E., Kusky, T.M., 2014. Geochronology of the Baye Mn oxide deposit, southern Yunnan Plateau: implications for the late Miocene to Pleistocene paleoclimatic conditions and topographic evolution. Geochem. Cosmochim. Acta 139, 227–247.
Drovetski, S.V., Semenov, G., Drovetskaya, S.S., Fadeev, I.V., Red'kin, Y.A., Voelker, G., 2013. Geographic mode of speciation in a mountain specialist avian family endemic to the Palearctic. Ecol. Evol. 3, 1518–1528.
Dickinson, E.C., 2003. The Howard & Moore Complete Checklist of the Birds, 3rd ed. Princeton University Press, Princeton.
Drovetski, S.V., Fadeev, I.V., Raković, M., Lopes, R.J., Boano, G., Pavia, M., et al., 2018. A test of the European Pleistocene refugial paradigm, using a Western Palaearctic endemic bird species. Proc. R. Soc. B 285, 20181606.
Drummond, A.J., Suchard, M.A., Xie, D., Rambaut, A., 2012. Bayesian phylogenetics with BEAUti and the BEAST 1.7. Mol. Biol. Evol. 29, 1969–1973.
Duchéne, S., Archer, F.I., Vilstrup, J., Caballero, S., Morin, P.A., 2011. Mitogenome phylogenetics: the impact of using single regions and partitioning schemes on topology, substitution rate and divergence time estimation. PLoS One 6, e27138.
Edwards, S.V., Xi, Z., Janke, A., Faircloth, B.C., McCormack, J.E., Glenn, T.C., et al., 2016. Implementing and testing the multispecies coalescent model: a valuable paradigm for phylogenomics. Mol. Phylogenet. Evol. 94, 447–462.
Esquerré, D., Ramírez-Alvarez, D., Pavón-Vázquez, C.J., Troncoso-Palacios, J., Garín, C.F., Keogh, J.S., et al., 2019. Speciation across mountains: phylogenomics, species delimitation and taxonomy of the *Liolaemus leopardinus* clade (Squamata, Liolaemidae). Mol. Phylogenet. Evol. 139, 106524.
Favre, A., Päckert, M., Pauls, S.U., Jähnig, S.C., Uhl, D., Michalak, I., et al., 2015. The role of the uplift of the Qinghai-Tibetan Plateau for the evolution of Tibetan biotas. Biol. Rev. 90, 236–253.
Fjeldså, J., Bowie, R.C.K., Rahbek, C., 2012. The role of mountain ranges in the diversification of birds. Annu. Rev. Ecol. Evol. Syst. 43, 249–265.
Ghalambor, C.K., Huey, R.B., Martin, P.R., Tewksbury, J.J., Wang, G., 2016. Are mountain passes higher in the tropics? Janzen's hypothesis revisited. Integr. Comp. Biol. 46, 5–17.
Gill, F., Donsker, D., 2016. IOC World Bird List, version 6.1. http://www.worldbirdlist.org/. (Accessed 20 December 2022).
Gill, F., Donsker, D., Rasmussen, P., 2022. IOC World Bird List, vol. 2. http://www.worldbirdnames.org/. (Accessed 20 December 2022).
González-Castellano, I., Pons, J., González-Ortegón, E., Marténez-Lage, A., 2020. Mitogenome phylogenetics in the genus *Palaemon* (Crustacea: Decapoda) sheds light on species crypticism in the rockpool shrimp *P. elegans*. PLoS One 15, e0237037.
Hatchwell, B.J., 2005. Family Prunellidae (accentors). In: Del Hoyo, J., Elliott, J., Christie, D.A. (Eds.), Handbook of the Birds of the World. Lynx Editions, Barcelona, pp. 496–513.
Hoang, D.T., Chernomor, O., von Haeseler, A., Minh, B.Q., Vinh, L.S., 2018. UFBoot2: improving the ultrafast bootstrap approximation. Mol. Biol. Evol. 35, 518–522.
Irisarri, I., Meyer, A., 2016. The identification of the closest living relative(s) of tetrapods: phylogenomic lessons for resolving short ancient internodes. Syst. Biol. 65, 1057–1075.
Katoh, K., Standley, D.M., 2013. MAFFT multiple sequence alignment software version 7: improvements in performance and usability. Mol. Biol. Evol. 30, 772–780.
Kohler, T., Maselli, D., 2009. Mountains and Climate Change – from Understanding to Action. Geographica Bernesia, Bern.
Kreft, H., Jetz, W., 2007. Global patterns and determinants of vascular plant diversity. P. Natl. Acad. Sci. USA 104, 5925–5930.
Lafon, C.W., 2004. High biodiversity: an assessment of mountain biodiversity. Divers. Distrib. 10, 75–76.
Lerner, H.R.L., Meyer, M., James, H.F., Hofreiter, M., Fleischer, R.C., 2011. Multilocus resolution of phylogeny and timescale in the extant adaptive radiation of *Hawaiian honeycreepers*. Curr. Biol. 21, 1838–1844.
Liu, B., Alström, P., Olsson, U., Fjeldså, J., Quan, Q., Roselaar, K.C.S., et al., 2017. Explosive radiation and spatial expansion across the cold environments of the Old World in an avian family. Ecol. Evol. 7, 6346–6357.
Maddison, W.P., Knowles, L.L., 2006. Inferring phylogeny despite incomplete lineage sorting. Syst. Biol. 55, 21–30.
Matzke, N.J., 2013. Probabilistic historical biogeography: new models for founder-event speciation, imperfect detection, and fossils allow improved accuracy and model-testing. Front. Biogeogr. 5, 242–248.
Matzke, N.J., 2014. Model selection in historical biogeography reveals that founder-event speciation is a crucial process in island clades. Syst. Biol. 63, 951–970.
Meng, G., Li, Y., Yang, C., Liu, S., 2019. MitoZ: a toolkit for animal mitochondrial genome assembly, annotation and visualization. Nucleic Acids Res. 47, e63.
Miao, Y., Herrmann, M., Wu, F., Yan, X., Yang, S., 2012. What controlled Mid-Late Miocene long-term aridification in Central Asia? –Global cooling or Tibetan Plateau uplift: a review. Earth Sci. Rev. 112, 155–172.
Mitchell, N., Lewis, P.O., Lemmon, E.M., Lemmon, A.R., Holsinger, K.E., 2017. Anchored phylogenomics improves the resolution of evolutionary relationships in the rapid radiation of Protea L. Am. J. Bot. 104, 102–115.
Meyer, M., Kircher, M., 2010. Illumina sequencing library preparation for highly multiplexed target capture and sequencing. Cold Spring Harb. Protoc. 6, prot5448.
Nguyen, L.T., Schmidt, H.A., von Haeseler, A., Minh, B.Q., 2015. IQ-TREE: a fast and effective stochastic algorithm for estimating maximum-likelihood phylogenies. Mol. Biol. Evol. 32, 268–274.
Oliver, J.C., 2013. Microevolutionary processes generate phylogenomic discordance at ancient divergences. Evolution 67, 1823–1830.
Philippe, H., Henner Brinkmann, H., Lavrov, D.V., Littlewood, D.T.J., Michael Manuel, M., Wörheide, G., et al., 2011. Resolving difficult phylogenetic questions: why more sequences are not enough. PLoS Biol. 9, e1000602.
Prum, R.O., Berv, J.S., Dornburg, A., Field, D.J., Townsend, J.P., Lemmon, E.M., et al., 2015. A comprehensive phylogeny of birds (Aves) using targeted next-generation DNA sequencing. Nature 526, 569–573.
Rambaut, A., 2012. FigTree Version 1.4.0. http://tree.bio.ed.ac.uk/software/figtree/. (Accessed 10 October 2020).
Ruggiero, A., Hawkins, B.A., 2008. Why do mountains support so many species of birds? Ecography 31, 306–315.
Song, G., Zhang, R., Alström, P., Irestedt, M., Cai, T., Qu, Y., et al., 2018. Complete taxon sampling of the avian genus *Pica* (magpies) reveals ancient relictual populations and synchronous Late-Pleistocene demographic expansion across the Northern Hemisphere. J. Avian Biol. 49, e01612.
Song, G., Zhang, R.Y., Machado-Stredel, F., Alström, P., Johansson, U.S., Irestedt, M., et al., 2020. Great journey of Great Tits (*Parus major* group): origin, diversification, and historical demographics of a broadly-distributed bird lineage. J. Biogeogr. 47, 1585–1598.
Stepanyan, L.S., 2003. Conspectus of the Ornithological Fauna of Russia and Adjacent Territories (Within the Borders of the USSR as a Historic Region). Academkniga, Moscow.
Svardal, H., Salzburger, W., Malinsky, M., 2021. Genetic variation and hybridization in evolutionary radiations of cichlid fishes. Annu. Rev. Anim. Biosci. 9, 55–79.

Swofford, D.L., 2021. PAUP* (Version PAUP* v.4.0a169). Phylogenetic Analysis Using Parsimony (*and Other Methods). http://phylosolutions.com/paup-test. (Accessed 5 January 2021).
Tarver, J.E., dos Reis, M., Mirarab, S., Moran, R.J., Parker, S., O'Reilly, J.E., et al., 2016. The interrelationships of placental mammals and the limits of phylogenetic inference. Genome Biol. Evol. 8, 330–344.
Wang, W., McKay, B.D., Dai, C., Zhao, N., Zhang, R., Qu, Y., et al., 2013. Glacial expansion and diversification of an East Asian montane bird, the green-backed tit (*Parus monticolus*). J. Biogeogr. 40, 1156–1169.
Yu, P., Zhou, L., Yang, W., Miao, L., Li, Z., Zhang, X., et al., 2021. Comparative mitogenome analyses uncover mitogenome features and phylogenetic implications of the subfamily Cobitinae. BMC Genom. 22, 50.
Yu, Y., Harris, A.J., Blair, C., He, X.J., 2015. RASP (reconstruct ancestral state in phylogenies): a tool for historical biogeography. Mol. Phylogenet. Evol. 87, 46–49.
Yu, Y., Harris, A.J., He, X., 2010. S-DIVA (statistical dispersal-vicariance analysis): a tool for inferring biogeographic histories. Mol. Phylogenet. Evol. 56, 848–850.
Zhang, Q., Ree, R.H., Salamin, N., Xing, Y., Silvestro, D., 2021. Fossil-informed models reveal a boreotropical origin and divergent evolutionary trajectories in the walnut family (Juglandaceae). Syst. Biol. 71, 242–258.
Zhang, R., Song, G., Qu, Y., Alström, P., Ramos, R., Xing, X., et al., 2012. Comparative phylogeography of two widespread magpies: importance of habitat of preference and breeding behavior on genetic structure in China. Mol. Phylogenet. Evol. 65, 562–572.
Zhao, M., Chang, Y., Kimball, R.T., Zhao, J., Lei, F., Qu, Y., 2019. Pleistocene glaciation explains the disjunct distribution of the chestnut-vented nuthatch (Aves, Sittidae). Zool. Scripta 48, 33–45.
Zhao, N., Dai, C., Wang, W., Zhang, R., Qu, Y., Lei, F., 2012. Pleistocene climate changes shaped the divergence and demography of Asian populations of the great tit *Parus major*: evidence from phylogeographic analysis and ecological niche models. J. Avian Biol. 43, 297–310.